

Optimal Design and Sizing of Solar-assisted CHP System Based on Thermodynamic and Economic Analysis

Fengyuan Wang, Yao Sheng, Linlin Liu*, Lei Zhang, Yu Zhuang, Jian Du

Institute of Chemical Process Systems Engineering, School of Chemical Engineering, Dalian University of Technology, Dalian 116024, Liaoning, China
 liulinlin@dlut.edu.cn

This work develops a method for the optimal design of a solar-assisted combined heat and power (CHP) system, in which the solar thermal central receiver subsystem and the steam power cycle subsystem are integrated to meet the real-time requirements of steam and power from production process. A mathematical model with the objectives of minimum total annual cost (TAC) and environmental impact (EI) is formulated to optimize the configuration and the size of the major equipment units, and schedule the dynamic operation of entire system. This model accounts for the hourly variability of Direct Normal Irradiance (DNI) and the electricity load in a typical day, as well as the power losses caused by the partial load operation of steam turbines. Based on the presented model, the optimum level of solar capacity is determined through a comprehensive analysis considering the trade-off between TAC and EI of the system. At last, a case study is illustrated and the results are elaborated to demonstrate that the desired system configuration can be obtained by application of the proposed model.

1. Introduction

With the increasing depletion of fossil fuels and the deterioration of environment, various clean energy sources as alternatives to fossil fuels are developed, in which solar energy, as an abundant and widely distributed renewable energy source, has attracted more and more attention (Abikoye et al., 2019). Sorgulu et al. (2018) proposed a solar tower-based energy system to produce electricity and fresh water, where the thermal energy storage tanks were considered to ensure power output in cloudy situations and at night, and the performance of the system has been discussed through energy analysis. Besagni et al. (2018) conducted an experimental test on an existing solar-assisted dual-source multifunctional heat pump to obtain the seasonal performances; in particular, energy and exergy analyses have been formulated based on experimental observations.

Compared to the systems driven solely by solar energy, the synergy of solar energy and fossil fuels can not only improve the thermal efficiency of the entire system, but also improve the ability to resist the output fluctuations caused by the intermittent nature of solar energy. Ocon et al. (2018) proposed a novel multi-criteria decision-making methodology for the selection of the most appropriate energy system for the off-grid electrification. Eight technology combination options were evaluated using six criteria covering socio-economic, environmental, and technical aspects. Results indicate that the fuel saver (diesel-solar PV hybrid) and diesel-solar PV-Li-ion hybrid systems yield the highest performance scores among the eight alternatives. Gutiérrez-Arriaga et al. (2013) presented a unified framework that combines process simulation with multi-objective optimization involving trade-off between annual profit and environmental impact (EI), while the types and amounts of primary energy sources as well as the optimal values of the operating conditions of the plant were optimized at the same time. Ponce-Ortega et al. (2011) presented a methodology for the energy integration of a system containing absorption refrigeration, which is driven by solar energy and other different types of heat sources.

The utility systems in chemical industry consume large amounts of fossil fuels every year. In previous studies, most of the researches on utility systems coupled with renewable energy and fossil fuels have focused on the analysis and evaluation for system with given structure, but few studies considered design problem for such system with variable heat and electricity demands and variable solar energy supply simultaneously. This study aims to launch the structure design and operating strategy optimization of a solar-assisted combined heat and power (CHP) system considering economic and environmental objectives. Typical structures of a solar-assisted

CHP system with and without energy storage unit are designed and optimized, which has also taken energy loss caused by variable energy demand and solar energy supply into account. In the CHP system, power and steam with defined pressure and temperature are generated through boiler and a set of turbines. Besides, solar energy is selected as a supplement to partially replace fossil fuel to drive utility systems, which effectively reduces EI. However, as the capital cost of the solar system is much higher than the utility system driven solely by fossil fuel, and the trade-off between total annual cost (TAC) and EI with different ratio of solar energy utilization is performed and a compromising system can be obtained to ensure the economic feasibility of the system on the premise that the EI meets the criterion. Corresponding mixed integer nonlinear programming (MINLP) mathematical model is formulated for optimal design purpose, and the case study is performed to illustrate the proposed method.

2. Superstructure

The integration of solar thermal central receiver subsystem and steam power cycle subsystem based on the superstructure is presented in Figure 1. In steam power cycle subsystem, the boiler consumes natural gas to generate the highest-level steam (VHP), part of which is used to directly meet the steam load, and the rest goes to multi-stage steam turbine expansion to generate power and lower-level steams including high-, middle- and low-pressure steams. In solar thermal central receiver subsystem, solar energy captured by cavity receiver fixed on the solar tower is used to heat the molten salt and thermal energy storage (TES) system consisting of high and low temperature molten salt storage tanks is considered (Sorgulu et al., 2018). In the steam generator, a part of the high temperature molten salt is used to generate VHP to reduce the load on boiler, and the rest is used to generate lower-level steams selectively along with turbine extraction to meet the remaining steam load. There are many factors related to the efficiency of multi-stage steam turbines. In order to reduce the difficulty in modelling, this study refers to the practice in Sun et al. (2015), which split a multi-stage turbine into a set of single-stage turbines which contains six back-pressure turbines and two condensing turbines. Binary variables are used to determine the existence of each single-stage turbine.

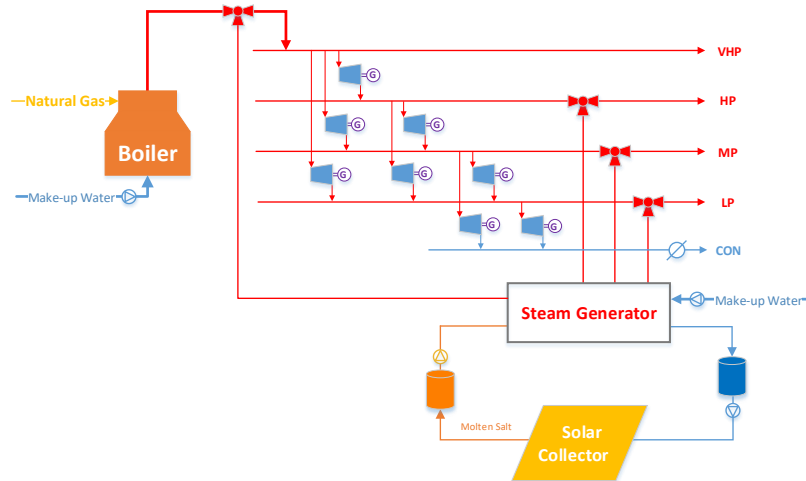


Figure 1: Superstructure for the solar-assisted CHP system with energy storage unit

3. Mathematical model

According to the superstructure proposed above, an MINLP mathematical model is formulated to assist the optimal design purpose of the study. The entire model consists of the both portions of central solar system and utility system, as well as the objective functions. Solver Baron in GAMS (Rosenthal, 2012) is employed to solve the model and obtain needed configuration. Then, ϵ -constraint method is introduced to launch the multi-objective optimization, where EI is set as constraint and TAC is set as objective function.

3.1 Model for central solar system

The total energy balance for the molten salt cavity receiver is given by Eq(1). Average receiver surface temperature is calculated by Eq(2) (Tehrani et al., 2016), which has an effect on the amount of energy loss on the receiver surface. Eq(3)-(6) denote energy loss caused by various mechanisms including radiation, reflection and convection (Li et al., 2010). The energy balance during the steam generation of molten salt is shown in Eq(7).

$$Q_{in,t} = Q_{abs,t} + Q_{loss,t} = A_{\text{heliostat}} \times I_{h,t} \times \eta_{\text{opt}} \times \text{HUR}_t \quad (1)$$

$$\frac{Q_{in,t}}{A_{re}} = (T_{re,t} - T_{\text{average}}) \left(\frac{d_{\text{outer}}}{d_{\text{inner}} \times h_{MS,t}} + \frac{d_{\text{outer}}}{2 \times \lambda_{\text{tube}}} \times \ln \frac{d_{\text{outer}}}{d_{\text{inner}}} \right) \quad (2)$$

$$Q_{loss,t} = Q_{\text{emission},t} + Q_{\text{reflection},t} + Q_{\text{convection},t} \quad (3)$$

$$Q_{\text{emission},t} = \varepsilon_{\text{average}} \times \sigma \times (T_{re,t}^4 - T_{\text{ambient}}^4) \times A_{\text{aperture}} \quad (4)$$

$$Q_{\text{reflection},t} = \rho \times Q_{in,t} \times VF \quad (5)$$

$$Q_{\text{convection},t} = h_{\text{force}} \times (T_{re,t} - T_{\text{ambient}}) \times A_{\text{aperture}} + h_{\text{nature},t} \times (T_{re,t} - T_{\text{ambient}}) \times A_{\text{receiver}} \quad (6)$$

$$Q_{abs,t} = m_{MS,t} \times C_{pMS} \times (T_H - T_L) = \sum_i \dot{m}_{\text{steam}_{i,t}}^{\text{solar}} \times \Delta H_i \quad (7)$$

Where λ_{tube} denotes the thermal conductivity of receiver tube, which takes a value of 23.9 W/(m·K); T_{average} and T_{ambient} are average temperature of molten salt in the receiver tube and ambient temperature; d_{inner} and d_{outer} are the inner and outer diameter of receiver tube; h_{MS} , h_{force} and h_{nature} denote the convection heat transfer coefficient of molten salt, forced convection and natural convection (Tehrani et al., 2016); subscripts i,t denote the steam level for utility system and hours in a day; heat conduction loss is ignored in Eq(3) because of its small proportion (Li et al., 2010).

3.2 Model for utility system design

Energy balance in boiler is given by Eq(8). Eq(9)-(10) denote the mass balance of steam. Eq(11) represents a linear formulation to determine performance of single-stage turbines (Aguilar et al., 2007).

$$QF_t \times \text{LHV} \times \text{EFF}_{\text{boiler}} = \dot{m}_{\text{steam}_t}^{\text{boiler}} \times \Delta H_{\text{VHP}} \quad (8)$$

$$\sum_i \dot{m}_{\text{steam}_{i,t}}^{\text{solar}} + \dot{m}_{\text{steam}_t}^{\text{boiler}} = \sum_i \dot{m}_{\text{steamload}_i} + \dot{m}_{\text{condensate}_t} \quad (9)$$

$$\sum_i \dot{m}_{\text{turbine}_{i,ip,t}} \times z_{i,ip} + \dot{m}_{\text{steam}_{ip,t}}^{\text{solar}} = \sum_{ip} \dot{m}_{\text{turbine}_{i,ip,t}} \times z_{i,ip} + \dot{m}_{\text{steamload}_{ip}} \quad (10)$$

$$W_{\text{turbine}_{i,ip,t}} = \Delta H_{i,ip} \times \frac{(Lst_{i,ip} + 1)}{Bst_{i,ip}} \times \dot{m}_{\text{turbine}_{i,ip,t}} - Lst_{i,ip} \times WED_{i,ip} - (Lst_{i,ip} + 1) \times \frac{Ast_{i,ip}}{Bst_{i,ip}} \quad (11)$$

Where $W_{\text{turbine}_{i,ip,t}}$ and denotes power generated via turbines; $\dot{m}_{\text{turbine}_{i,ip,t}}$ denotes steam mass flow in turbines; $\dot{m}_{\text{steam}_{i,t}}^{\text{solar}}$ and $\dot{m}_{\text{steam}_t}^{\text{boiler}}$ denote the steam generated via steam generator and boiler; A_{st} , B_{st} and L_{st} are regression coefficients; $WED_{i,ip}$ denotes the rated power of a single-stage steam turbine.

3.3 Objective function

In this study, the TAC and the EI of the solar-assisted CHP system are simultaneously minimized to guide the system design. As indicated in Eq(12)-(14), the TAC is composed of capital cost (CAPC) and operating cost (OPEC). The operating cost is the sum of fuel cost and solar field maintain cost.

$$\min \text{TAC} = \text{CAPC} + \text{OPEC} \quad (12)$$

$$\text{CAPC} = C_{\text{heliostat}} \times A_{\text{heliostat}} + FC_{\text{solar}} + C_{\text{SG}} \times (Q_{\text{abs},t})_{\text{MAX}} + \text{CAPC}_U \quad (13)$$

$$\text{OPEC} = \sum_t C_{\text{NG}} \times QF_t + C_M \times \sum_t Q_{\text{abs},t} \quad (14)$$

EI is measured by Greenhouse gas (GHG) emissions, which is related to the extraction and combustion of natural gas (Gutiérrez-Arriaga et al., 2013).

$$\min \text{EI} = GE_{\text{NG}} \times \text{LHV} \times \sum_t QF_t \times EC_{\text{climate}} + \sum_t QF_t \times EC_{\text{resource}} \quad (15)$$

Where $C_{\text{heliostat}}$ and C_{SG} are the unit capital cost of heliostat and steam generator; CAPC_U is the capital cost of main equipment units of the steam power cycle; FC_{solar} is the fixed capital cost of solar tower and receiver; C_{NG} and C_M are the units operating costs for natural gas and heliostat field maintenance; GE_{NG} denotes GHG

emission; $E_{C_{climate}}$ and $E_{C_{resource}}$ denote the eco-indicator related to damage caused by GHG emissions and extraction of natural gas.

3.4 Model for the solar-assisted CHP system considering energy storage

When energy storage system is considered, the energy storage cost should be added into the CAPC. Eq(17) is used to determine the corresponding molten salt storage tank capacity under a specified heliostat field area.

$$CAPC = C_{heliostat} \times A_{heliostat} + FC_{solar} + C_{SG} \times (Q_{abs,t})_{MAX} + CAPC_{storage} + CAPC_U \quad (16)$$

$$V_H = \max \left[(m_{H,in,1} - m_{H,out,1}), \sum_{h=1}^2 (m_{H,in,h} - m_{H,out,h}), \sum_{h=1}^3 (m_{H,in,h} - m_{H,out,h}), \dots, \sum_{h=1}^{24} (m_{H,in,h} - m_{H,out,h}) \right] / \rho_{ms} \times \varphi \quad (17)$$

4. Case study

A case study is presented in this section to illustrate the proposed method. Irradiation on an hourly basis is considered for a specific day in a typical summer month (Abikoye et al., 2019). The steam mains and demands are given in Table 1 and the hourly power demands are given in Table 2. Other parameters used in this study include: the price and heating value of natural gas are 0.8552 \$/kg and 54.0 MJ/kg (Gutiérrez-Arriaga et al., 2013); the temperatures of the molten salt at the inlet and outlet of the cavity receiver are 559 K and 838 K (Tehrani et al., 2016); $C_{heliostat}$, C_{SG} and C_M are specified with 126 \$/m², 300 \$/kW_e and 0.012 \$/kWh (Li et al., 2019); the optical efficiency of heliostat field and burn efficiency of the boiler are set as 0.6 and 0.98.

Table 1: Steam mains and demands data

Steam main	VHP	HP	MP	LP
Pressure(MPa)	10.1	2.06	0.41	0.27
Temperature(°C)	539	333	186	150
Demands(t/h)	30	60	40	50

Table 2: Power demands data

Time(h)	0	1	2	3	4	5	6	7	8	9	10	11
Power demand (kW)	15,075	15,237	15,412	15,745	15,970	15,969	16,370	15,172	12,360	11,615	12,974	14,060
Time(h)	12	13	14	15	16	17	18	19	20	21	22	23
Power demand(kW)	14,554	15,019	14,003	13,287	13,047	13,540	10,298	8,640	10,638	13,164	14,411	14,427

For the solar thermal central receiver subsystem studied in this paper, two situations are investigated for comparative analysis. Energy storage is not considered in the first situation (Structure 1), so molten salt absorbs solar energy as heat transfer fluid and directly enters the steam generator as heat sources to produce steam in real time; the other structure contains an energy storage unit (Structure 2), and the molten salt is heated to the specified temperature in the cavity receiver and sent to the high-temperature storage tank firstly, then the stored molten salt can be assigned to the steam generator for steam generation according to the real-time fluctuating energy demand. Both structures are presented into MINLP models and solved using BARON in GAMS with near-optimal solutions obtained.

Figure 2 shows the economic-environment multi-objective curves corresponding to the two structures. The left and right endpoints in the curve are calculated using the EI and TAC as the single objective function (the left endpoint of Structure 2 is omitted for reason of rationality). The intermediate points are obtained by taking equal step EI value as the upper boundary constraint and minimizing the TAC. It can be seen from Figure 2 that the two curves on the right side almost overlap with environmental constraints increasing. At this area, the energy storage unit in Structure 2 does not exist, and there is no obvious difference between Structure 1 and 2. The reason is that solar energy in this area can be fully utilized at any time of the day, so the energy storage unit has no extra contribution to the improvement of economic performance. With the decrease of EI constraints, the economic advantage of Structure 2 grows greater.

Points with the same EI in both structures are selected (EI=1.17×10⁶ Ec) to analyse the performance of the two systems within one day. Table 3 shows the economic comparison of these two structures, including TAC, CAPC, $A_{heliostat}$, $CAPC_{storage}$ and OPEC. As it can be seen, the heliostat field area required for Structure 2 to achieve the same EI is greatly reduced, which leads to a significant reduction in capital cost. At the same time, the additional cost of energy storage is negligible, so the TAC of Structure 2 has been significantly reduced. Figure

3a shows the hourly steam generation at the specified EI. Correspondingly, Figure 3b shows hourly steam generation for Structure 2 under the same EI. As indicated, in Structure 2, solar energy not only drives the utility system during periods of sufficient irradiation, but also generates low pressure steam by releasing energy stored in the energy storage unit during low irradiation periods to partially meet the steam demand.

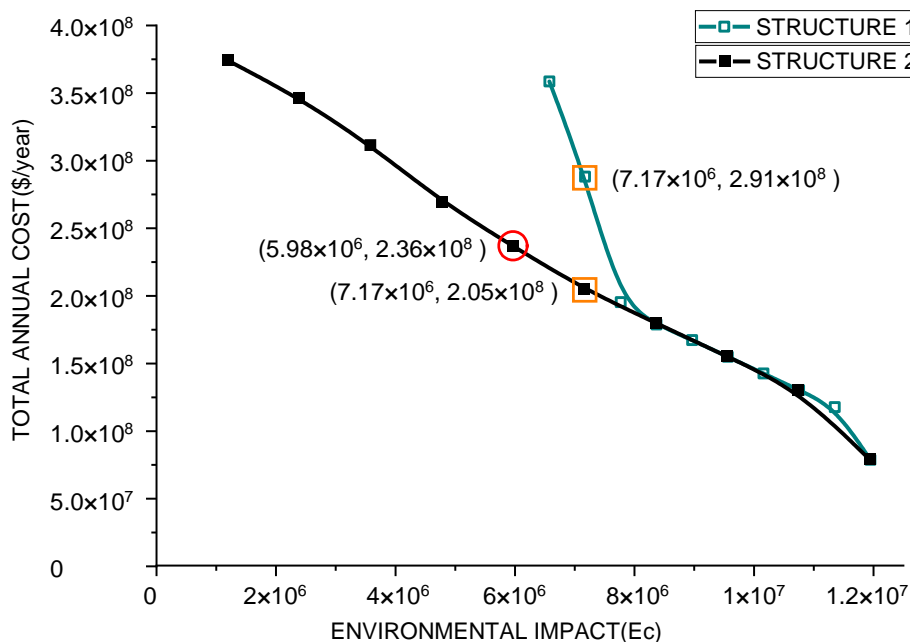


Figure 2: Pareto curves for structure 1 and Structure 2

With the decrease of EI constraint, the scale of solar subsystem in Structure 1 must increase greatly to absorb sufficient solar energy during periods of low irradiation to meet the environmental constraints, however, the utilization of solar energy at noon is insufficient, leading a waste. This part of energy can be effectively stored and released when needed in Structure 2, which can effectively reduce the scale of solar thermal central receiver subsystem under the same EI, accordingly, the initial investment cost of equipment is reduced as well.

Finally, the optimal design point is obtained on the multi-objective curve corresponding to Structure 2 (EI = 5.98×10^6 Ec). Both TAC and EI take reasonable values at this point. The heliostat field area is 61.9 ha, and the required molten salt quality is 524.8 t.

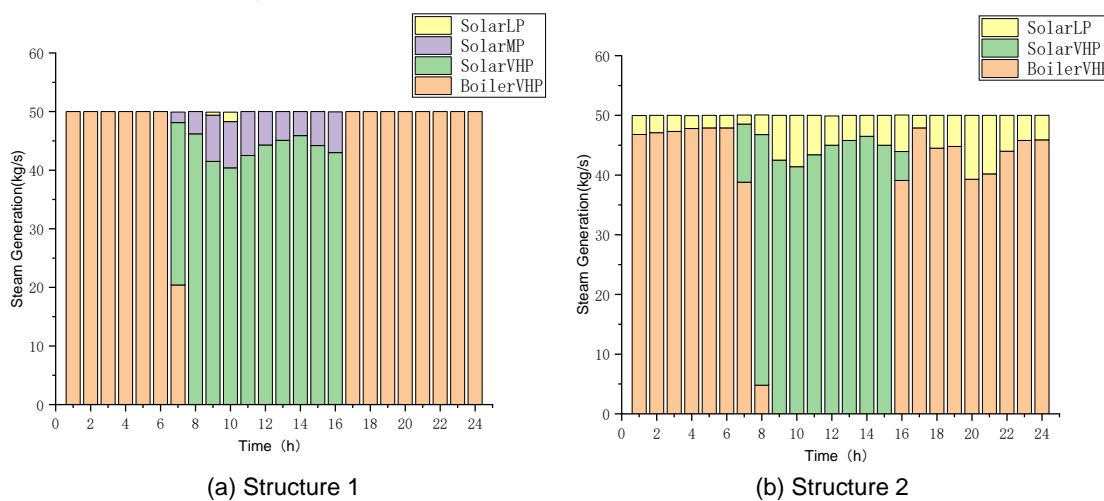


Figure 3: Steam generation

Table 3: Economic comparison between Structure 1 and Structure 2

	TAC(\$/y)	CAPC(\$)	A _{heliostat} (ha)	CAP _{storage} (\$)	OPEC(\$/y)
Structure1	2.91×10^8	2.38×10^8	128.60	0	5.30×10^7
Structure2	2.05×10^8	1.52×10^8	49.40	4.40×10^6	5.28×10^7

5. Conclusions

This paper has developed a multi-objective optimization method for a solar-assisted CHP system to realize the trade-off between the TAC and EI. Optimal structure of CHP system is designed considering the energy loss caused by fluctuation of energy demands and solar energy supply. The systems with and without energy storage units are both studied based on the method, with the operating strategy determined simultaneously according to the variation of solar irradiation and power demands. The multi-objective optimization is launched to investigate the influence of solar subsystem scale on TAC and EI of the overall system. Results show that energy storage units are necessary when there is greater demand for EI reduction, because they will help to reduce the cost of the system. But if the solar subsystem is in smaller scale, the two systems have almost the same performance in economic and environmental aspects. The optimal point is obtained by making a trade-off between TAC and EI, where the values of TAC and EI are 2.36×10^8 \$/y and 5.98×10^6 Ec. In the future, works will be aimed at optimal designs of the obtained system under uncertainty.

Acknowledgements

The authors gratefully acknowledge the financial support from "Natural Science Foundation of China" (No. 21878034) and the Fundamental Research Funds for Central Universities of China (DUT18LAB11).

References

- Sorgulu F., Dincer I., 2018, Design and analysis of a solar tower power plant integrated with thermal energy storage system for cogeneration, *International Journal of Energy Research*, 43, 6151–6160.
- Besagni G., Croci L., Nesa R., 2018, Solar-assisted dual-source multifunctional heat pump: field tests results and thermodynamic analysis, *Chemical Engineering Transactions*, 70, 253-258.
- Ocon J.D., Cruz S.M.M., Castro M.T., Aviso K.B., Tan R.R., Promentilla M.A.B., 2018, Optimal multi-criteria selection of hybrid energy systems for off-grid electrification, *Chemical Engineering Transactions*, 70, 367-372.
- Gutiérrez-Arriaga C.G., Serna-González A.M., Ponce-Ortega J.M., El-Halwagi M.M., 2013, Multi-objective optimization of steam power plants for sustainable generation of electricity, *Clean Technologies And Environmental Policy*, 15, 551-566.
- Ponce-Ortega J.M., Tora E.A. González-Campos J.B., El-Halwagi M.M., 2011, Integration of renewable energy with industrial absorption refrigeration systems: systematic design and operation with technical, economic, and environmental objectives, *Industrial & Engineering Chemistry Research*, 50, 9667-9684.
- Sun L., Smith R., 2015, Performance modeling of new and existing steam turbines, *Ind. Eng. Chem. Res.*, 54, 1908-1915.
- Aguilar O., Perry S.J., Kim J.K., Smith R., 2007, Design and optimization of flexible utility systems subject to variable conditions, *Chemical Engineering Research and Design*, 85(A8), 1136-1148.
- Li X., Kong W., Wang Z., Chang C., Bai F., 2010, Thermal model and thermodynamic performance of molten salt cavity receiver, *Renewable Energy*, 35, 981-988.
- Rosenthal R.E., 2012. *GAMS-A User's Guide*. GAMS Development Corporation, Washington DC, United States.
- Abikoye B., Isafiade A.J., Kravanja Z., 2019. Integrated design for direct and indirect solar thermal utilization in low temperature industrial operations, *Energy*, 182, 381-396.
- Tehrani S.S.M., Taylor R.A., 2016, Off-design simulation and performance of molten salt cavity receivers in solar tower plants under realistic operational modes and control strategies, *Applied Energy*, 179, 698-715.
- Li C., Zhai R., Yang Y., Patchigolla K., Oakey J.E., Tumer P., 2019, Annual performance analysis and optimization of a solar tower aided coal-fired power plant, *Applied Energy*, 237, 440-456.